Available online at www.sciencedirect.com
SCIENCE DIRECT
ELSEVIER
Polymer 46 (2005) 7118–7131
polymer
www.elsevier.com/locate/polymer

Mesoglobules of thermoresponsive polymers in dilute aqueous solutions above the LCST

Vladimir Aseyev[a,*], Sami Hietala[a], Antti Laukkanen[a], Markus Nuopponen[a], Ondine Confortini[b], Filip E. Du Prez[b], Heikki Tenhu[a]

[a]*Laboratory of Polymer Chemistry, University of Helsinki, PB 55, FIN-00014 HY Helsinki, Finland*
[b]*Department of Organic Chemistry, Polymer Chemistry Research Group, Ghent University, Krijgslaan 281, S4, B-9000 Gent, Belgium*

Received 7 October 2004; received in revised form 15 March 2005; accepted 9 May 2005
Available online 14 June 2005

Abstract

The colloidal stability and characteristics of particles formed by homopolymers of poly(*N*-vinyl caprolactam), poly(*N*-isopropyl acrylamide) and poly(vinyl methyl ether) in dilute aqueous solutions above the lower critical solution temperature, LCST, was followed by means of dynamic and static light scattering. Depending on the solution concentration, the homopolymers precipitate or form stable dispersions of monodisperse spherical particles. To obtain colloidally stable aggregates, also called mesoglobules, no stabilising agent was added. The stability of the mesoglobules upon time and dilution at temperatures above the LCST suggests that the particle surfaces possess a hydrophilic character. The size of the formed particles depends on the concentration and the heating rate of the solutions. However, internal structure and shape of mesoglobules are affected neither by the way, how the mesoglobules were prepared, nor by molar mass of individual macromolecules. Mesoglobules of PNIPAM obey the $M \propto R^{2.7}$ scaling law. Origin of stability of the dispersions vs. expected precipitation is discussed.

Keywords: Thermally responsive polymer; Aggregate; Mesoglobule

1. Introduction

Thermo-responsive homopolymers poly(*N*-isopropyl acrylamide), PNIPAM [1,2], and poly(*N*-vinyl caprolactam), PVCL [3,4], are widely studied and used polymers. In contrast, smaller number of studies has been carried out on the other thermosensitive polymer, poly(vinyl methyl ether), PVME [5–9]. Our recent observations on thermal behaviour of aqueous solutions of these polymers require a short overview of existing results in order to understand the formation of stable aggregates without any foreign stabilising agents.

These polymers are soluble in cold water and phase separate upon heating above the lower critical solution temperature, LCST. The cloud point temperature of aqueous PNIPAM solutions is above 31 °C regardless of the molar mass of the polymer [1,2]. For aqueous PVCL solutions, the cloud point is above 30 °C, although it increases with decreasing the molar mass of PVCL [3]. Poly(vinyl methyl ether), PVME, is known to cloud in water at temperatures 32–40 °C depending on polymer molar mass and concentration [5]. Despite of the apparent similarity, these polymers show three different types of demixing based on a general phenomenological analysis of the critical miscibility with water: PVCL belongs to Type I [4], PNIPAM to Type II [2], and PVME to Type III [6]. Polymers of the Type I follow the classical Flory–Huggins behaviour meaning that the liquid–liquid critical composition shifts towards lower polymer concentrations upon increasing polymer molar mass. Critical composition does not change with polymer molar mass for the polymers of the Type II. Phase diagrams of the polymers of the Type III are bimodal with two critical points at low and at high polymer concentrations representing Type I and Type II behaviour respectively.

At the phase separation boundary, thermoresponsive

* Corresponding author. Tel.: +358 9 191 50335; fax: +358 9 191 50330.
E-mail address: vladimir.aseyev@helsinki.fi (V. Aseyev).

0032-3861/$ - see front matter © 2005 Elsevier Ltd. All rights reserved.
doi:10.1016/j.polymer.2005.05.097

polymers undergo the coil-to-globule transition upon heating. To investigate the coil-to-globule transition on molecular level, one should study extremely dilute solutions of high molar mass samples to overcome a strong tendency of macromolecules to aggregate. A number of studies on the coil-to-globule transition have been done on aqueous solutions of a single PNIPAM chain ($M_w = 10^7$ g/mol) using light scattering methods [10,11]. Light scattering from aqueous PVCL solutions ($M_w \sim 10^6$ g/mol) has also been studied in the vicinity of the phase transition boundary [12]. Observation of the coil-to-globule transition of PVCL ($M_w \sim 10^6$ g/mol) in D_2O by small angle neutron scattering has recently been reported [13,14]. Latter study was performed at the threshold of the polymer overlap concentration c^*.

What happens in a dilute, though not extremely dilute, solution of thermosensitive polymers with moderate molar masses above the LCST? The solutions look cloudy, which generally is understood as a microscopic phase separation. The microscopically separated phase is expected to be metastable and the polymers should gradually precipitate. However, the formation of dense mesoscopic globules, mesoglobules, in PNIPAM homopolymer ($M_w = (0.5–10) \times 10^6$ g/mol) solutions has been reported [15–18]. Mesoglobules are equally sized spherical aggregates of more than one and less than all polymer chains colloidally stable in solution [18]. PNIPAM dispersions of polymer concentration below 0.2 g/l at 55 °C were studied by light scattering [15] and the formed particles/mesoglobules had a narrow size distribution. The size of the particles was found to increase with increasing the polymer concentration and decreasing heating rate. Colloidal stability of polymer solutions was understood in terms of spinodal decomposition above the LCST and low probability of Brownian collisions in dilute solutions [16]. Thus, the polymer in poor solvent optimises its interaction energy via the intermolecular association between polymer chains and at the same time the translational entropy of the chains decreases. When these two energy terms are compensated, the adopted metastable state yields polymeric mesoglobules. The theory of mesoglobule formation has been developed and applied for block and random heteropolymers [19,20].

Typically, colloidal stability is achieved by modification of the surface of the intermolecular aggregates sterically [21,22] or electrostatically [23–26]. Electrostatically stabilized PNIPAM aggregates (0.01–1.0 g/l) have been obtained by the addition of sodium dodecyl sulphate, SDS [23]. It has recently been observed that introduction of positively [24,25] or negatively [26] charged comonomers leads to the formation of stable aggregates at temperatures higher than the LCST as well. Steric stabilization may be achieved by the coverage of the surface of the aggregates by uncharged hydrophilic substances. For PNIPAM grafted with poly (ethyleneoxide), PEO, sterically stabilised spherical particles above the LCST have been reported [21,22]. Copolymerization of NIPAM with hydrophilic vinylpyrrolidone, VP, at temperatures above and below its LCST results in segmented and random distribution of VP units, respectively [27]. The copolymers with a segmented VP distribution aggregate more readily upon heating and form stable aggregates larger than those with a random VP distribution.

Amphiphilic polymers, remaining soluble in aqueous medium after the transition to the globular state, mimic globular proteins and have been called protein-like polymers [28–30]. The main features of all globular proteins are that they are globular but do not precipitate in aqueous medium. Hydrophobic repeating units of a protein form a core of the globule whereas hydrophilic and charged units form the shell around this core. Preparation of synthetic protein-like copolymers is difficult, which explains a small number of publications in this field. All the known studies deal with copolymers based on thermoresponsive PNIPAM [21,22,27] and PVCL [25].

Competition of the hydrophobic and hydrophilic effects in respect to the phase behaviour of thermosensitive polymers in water has been studied using both mean-field theoretical methods and computer simulations [31–33]. The simplest HP side-chain model of an amphiphilic polymer consisting of hydrophobic, H, and hydrophilic, P, beads was analysed. In this model, the dualistic character of each repeating unit is expressed as an H bead forming a hydrophobic backbone and a P bead representing a hydrophilic side group [33]. When an amphiphilic macromolecule collapses, the hydrophobic backbone folds, whereas the hydrophilic groups turn outside towards the water molecules. The macromolecule adopts an intermediate necklace-like conformation where hydrophilic groups surround single pearls of hydrophobic groups. Stretched chain sections interconnect pearls. Reducing of thermodynamic quality of the solvent results in increasing size of pearls and decreasing their number. Finally, the pearls coalesce and form a cylindrical particle [33].

According to the mechanism described above, an amphiphilic macromolecule in a fully collapsed/globular state may be colloidally stable without any foreign stabilising agents, such as charges or hydrophilic comonomers or detergents. Obviously, to form a stable particle, the outer shell of the particle should be hydrophilic. In this respect, the formation of cylindrical globule is preferable owing to the large surface to volume (or molar mass) ratio. However, existence of a cylindrical globule formed by amphiphilic polymers has not been observed in a real experiment so far.

Regardless of the considerable interest on the amphiphilic polymers, experimental studies on colloidally stable mesoglobules formed by the thermoresponsive homopolymers above the LCST are few [15–17]. All of them deal with PNIPAM mesoglobules. Moreover, PNIPAM samples have been synthesised by free-radical polymerisation using ammonium persulfate as an initiator. Despite of the small number of ionic end-groups of PNIPAM, these charges may

be situated on the surface of the PNIPAM mesoglobules and thus significantly contribute to the stability. Moreover, as stated above, there are at least three types of thermoresponsive polymers and mesoglobular state of PNIPAM may be not a universal phenomenon. Up today, there is only one known report on mesoglobules formed by PVCL [34]. It is essential that in that report the PVCL samples were synthesised using a neutral initiator.

In this report we summarize our observations on mesoglobules formed by thermoresponsive PVCL, PNIPAM and PVME homopolymers bearing neutral end groups. Molar masses ($M_w \sim 10^4$–10^5 g/mol) are significantly lower than those for PNIPAM samples reported earlier [15–17]. As previously was stated [16], formation of mesoglobules is limited for the polydisperse polymers. Our studies suggest that high molar mass chains in poor solvent adopt a single chain globular conformation, whereas the low molar mass samples form spherical monodisperse mesoglobules, the size of which is not significantly affected by the molar mass of individual chains. Solution behaviour of thermoresponsive *block*-copolymers polymers is discussed. Special attention is paid to the shape of the mesoglobules. Cylindrical vs. spherical models of mesoglobules are discussed.

2. Experimental

2.1. Materials

N-Isopropylacrylamide (NIPAM, Polysciences, Ins.) and *N*-vinylcaprolactam (VCL, Aldrich Chemicals) were purified by recrystallisation from benzene. 2,2′-Azo-bis-isobutyronitrile (AIBN, Aldrich Chemicals) was recrystallised from methanol. 2,2′-Azo-bis[-2-methyl-*N*-(2-hydroxyethyl) propionamide] (VA-086, Wako Chemicals) was used as received. Vinyl methyl ether (VME, BASF) was dried through a CaH_2 trap. For PVME synthesis, HPLC grade toluene and anhydrous diethyl ether were distilled over sodium prior to use in the presence of traces of benzophenone as indicator of H_2O. Zinc iodide (ZnI_2) (Aldrich 99.99%) was dried under vacuum for 12 h before use. Tetrahexylaluminium (THA) (Interspe Hamann Group) was dissolved in dry toluene (0.1 M). Trimethylsilyl iodide (TMSI) (Aldrich 97%, 5 ml ampoule), anhydrous sodium thiosulfate ($Na_2S_2O_3$) (Aldrich 99%) and lithium borohydride ($LiBH_4$) (Acros Organics), a 2 M solution in tetrahydrofurane, were used as received. 1,1,3,3-tetramethoxypropane (TMoP) (bp = 183 °C, Acros Organics 99%) was purified by refluxing 4 h and distilled over CaH_2 under reduced pressure. THA and TMoP were stored under argon at low temperature. All glassware was dried for at least 24 h in a drying oven at 70 °C. Deionised water was received from an Elgastat UHQ-PS water purification system.

2.2. Synthesis

Chemical structures of PNIPAM, PVCL and PVME are shown in Fig. 1 and molecular characteristics are presented in Table 1.

To prepare poly(*N*-isopropyl acrylamide), PNIPAM, of $M_w = 27300$ g/mol, NIPAM (83,6 mmol, 10 mass%), chain transfer agent 2-aminoethanethiol hydrochloride (AESH, 124 mg, 1.3 mol%) and AIBN (24 mg, 0.1 mol%) were dissolved in DMF (100 ml). Before addition of AIBN the reaction vessel was flushed with nitrogen for 45 min. The vessel was placed in an oil bath at 70 °C and kept at that temperature for 22 h. PNIPAM was precipitated in diethyl ether. PNIPAM with $M_w = 160{,}000$ g/mol was prepared by free radical polymerisation in dioxane as previously reported [35].

Poly(*N*-vinyl caprolactam), PVCL, samples were prepared by radical polymerisation using either benzene or toluene as a solvent, as reported previously [34]. Similar to PNIPAM, a non-ionic radical initiator, AIBN, was used to initiate the polymerisations. PVCL samples were purified using extensive reprecipitation and dialysis.

Two samples of poly(vinyl methyl ether), PVME, have been synthesized using a living cationic polymerisation. The polymerisation was carried out in toluene with a 1,1,3,3-tetramethylmethoxypropane/trimethylsilyl iodide, TMoP/TMSI, as initiator and zinc iodide, ZnI_2, as activator, which is known to produce living vinyl ether polymerisations [36]. A semi-continuous process for the polymerisation of PVME has been described elsewhere [37]. At −5 °C and using an activator/initiator ratio of 1/33 with the presence of tetrahexyl aluminium, THA, the conversions were almost quantitative, i.e. controlled molar masses and low polydispersity. Termination of these homopolymers with lithium borohydride, $LiBH_4$, leads to a stable hydrogen end group. The quenched reaction mixture was washed with 10% aqueous sodium thiosulfate solution ($Na_2S_2O_3$), then with deionized water, and dried over anhydrous $MgSO_4$, and then under reduced pressure.

Amphiphilic diblock copolymers of poly(*N*-isopropyl acrylamide)-*block*-polystyrene, PNIPAM-*b*-PS, and poly(*N*-isopropyl acrylamide)-*block*-poly(*tert*-butyl methacrylate), PNIPAM-*b*-P*t*BMA, with low polydispersities were synthesized using RAFT reactions. Details of synthesis can be found elsewhere [38]. PNIPAM was used as a hydrophilic block, and either PS or P*t*BMA as the

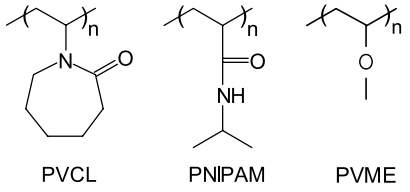

Fig. 1. Chemical structures of poly(*N*-vinyl caprolactam), PVCL, poly(*N*-isopropyl acrylamide), PNIPAM, and poly(vinyl methyl ether), PVME.

Table 1
Molecular characteristics of polymers studied

Polymer	M_w SEC, (g/mol)	M_n SEC, (g/mol)	M_w/M_n	SEC conditions	M_w SLS[a], (g/mol)	M_n ^{1}H NMR, (g/mol)
PNIPAM	27,300	15,500	1.76	THF/PS		
PNIPAM					160,000	
PVCL					30,000	
PVCL					330,000	
PVME	12,800	9400	1.36	Chloroform/PS		7100
PVME	19,600	14,000	1.40	Chloroform/PS		12,000
PNIPAM-*b*-PS[b]	24,800	21,600	1.15	THF/PS		
PNIPAM-*b*-P*t*BMA[c]	37,600	33,300	1.13	THF/PS		

[a] Weight average molar masses of individual macromolecules in organic solvents.
[b] M_n of PNIPAM block is 13,600 and of PS is 8000; 62 mol% of PNIPAM.
[c] M_n of PNIPAM block is 13,900 and P*t*BMA is 19,400; 47 mol% of PNIPAM.

hydrophobe. The diblock copolymers form micellar structures in water when carefully transferred from an organic solvent (DMA as a solvent common for both blocks) into aqueous solution. Deionised water was added dropwise to the solutions with vigorous stirring. 15–25 wt% of water was added depending on the polymer. The quality of the solvent became gradually poorer for the hydrophobic blocks, thus causing the aggregation of the hydrophobic blocks observed as the turbidity of the solutions. The resulting slightly opaque solutions were placed in dialysis bags (Cellu Sep T1, nominal MWCO:3500) and dialysed against purified water to remove DMA.

2.3. Analytical techniques

The purity of the synthesized polymers was ascertained by ^{1}H NMR spectroscopy using a Bruker AC 500 FT NMR for PVME samples and using a 200 MHz Varian Gemini 2000 spectrometer for all the other polymers.

Dynamic, DLS, and static, SLS, light scattering experiments were performed to investigate properties of intermolecular aggregates on nanometer scale. Methodological aspects of DLS can be found elsewhere [39]. DLS and SLS light scattering experiments were performed using a Brookhaven Instrument BIC-200 SM goniometer and BIC-9000 AT digital correlator. An Argon ion laser (LEXEL 85, 1 W) operating at 514.5 nm wavelength was used as a light source, the laser power being typically ~25 mW. PVME was studied using a He/Ne laser (Spectra Physics SP127-35, ~20 mW) operating at 632.8 nm. In DLS experiments, autocorrelation functions of intensity of scattered light, $G_2(t)$, were collected at scattering angles ranging between 20 and 150°. Simultaneously, time average intensity of scattered light, I, was recorded. Intensities measured in counts of photons per second were normalised with respect to the Rayleigh ratio of toluene. The measurement temperature ranged from 10 to 50 °C was controlled by means of a Lauda RC 6C thermostat. Solutions were purified of dust using Millex PVDF 0.45 m filter units.

The molar masses of the polymers were determined by SLS and by size exclusion chromatography, SEC. A Waters liquid chromatography system was equipped with a Waters 2410 refractometer and three Styragel columns (HR2, HR4, HR6). For PVME analysis, a Waters instrument was equipped with a 60 cm 1000 Å column (Polymer Laboratories) and a Melz refractometer. Analysis was performed at room temperature with chloroform or THF as eluent and 0.8 ml/min flow rate. The molar masses were determined against polystyrene standards (PS, Polymer Laboratories), see Table 1.

High sensitivity differential scanning calorimetry, HS DSC, measurements were performed for aqueous polymer solutions with a VP-DSC microcalorimeter (MicroCal Inc) at an external pressure of ca. 180 kPa. The cell volume was 0.507 ml. The instrument response time was set at 5.6 s. Scans were performed from 10 to 100 °C at heating rates of 30, 60, and 90 °C h^{-1}. Prior to each scan the sample was kept at 10 °C for 15 min. Data were corrected for instrument response time and analysed using the software supplied by the manufacturer. The heat of transition, ΔH, is given in kJ/mol of repeating units. For PNIPAM and PVME, $\Delta C_p = C_p(50\,^\circ\mathrm{C}) - C_p(15\,^\circ\mathrm{C})$ and for PVCL, $\Delta C_p = C_p(90\,^\circ\mathrm{C}) - C_p(25\,^\circ\mathrm{C})$.

Pressure perturbation calorimetry, PPC, measurements were performed on a VP-DSC microcalorimeter equipped with a pressure perturbation accessory (MicroCal Inc). The reference cell and sample cell volumes were identical (0.507 ml). The polymer concentration was 5.0 g l^{-1}. Additional information on the PPC technique and the method is presented elsewhere [34,40,41].

2.4. Preparation of polymer solutions

Homopolymers were dissolved in ultra pure water (ELGA PURELAB Ultra DV 35) overnight at room temperature and then diluted to concentrations ranging from 0.02 to 0.25 g/l. Two PVME solutions of 0.02 and 1.00 g/l concentration were studied. Polymeric micelles formed by block copolymers were studied in aqueous

solutions of 0.20 g/l. Solutions were kept at room temperature at least for 24 h prior to measurements.

Two different heating schemes were applied in the light scattering experiments. In the equilibrium heating scheme, light scattering cuvettes containing 2.0 ml of solutions were heated slowly, i.e. stepwise, from 20 to 50 °C in 2–5 °C steps allowing one hour in average for equilibration at each temperature. Stability of intensity of scattered light was a criterion showing that a solution reached equilibrium. In the non-equilibrium heating scheme, the samples were transferred from room temperature straight into the oven at 50 °C. The solutions were kept at 50 °C for several weeks in order to follow the colloidal stability of the samples. The possible precipitation was inspected visually as well as using intensity of scattered light.

The effect of dilution at 50 °C on size of the mesoglobules was studied. To dilute the solutions, the light scattering cuvettes containing 2.0 ml of concentrated dispersion were kept at 50 °C while a known amount of filtered hot water was added consequently. The hydrodynamic size and intensity of scattered light were measured after the intensity was stabilized.

3. Results

The PNIPAM polymers visually precipitate from solutions with concentrations above 1.00 g/l when heated above the LCST. Redissolving the samples at room temperature and reheating them above the LCST resulted in similar behaviour. For both PVCL polymers, no precipitation was observed in the solutions with concentration below 0.25 g/l. Visually, behaviour of PVME is similar to PNIPAM. Taking into account a small number of reports on aqueous PVME in vicinity of its LCST we shall pay special attention to this polymer in this publication.

Molar masses of PVME samples studied are low and scattering intensity from the solutions of polymer concentrations smaller than 1.00 g/l is weak below the LCST. Therefore, distributions of hydrodynamic radius cannot be obtained with sufficient accuracy. On the other hand, scattering from 1.00 g/l solution heated above the LCST is too strong and consists of multiple scattering. The latter effect is especially noticeable at scattering angles lower than 70–60°. This leads to incorrect values of R_g and R_h and only qualitative analysis of the experimental data is possible. Therefore, at 20 °C, light scattering from the PVME samples was studied in aqueous solutions with 1.00 g/l polymer concentration, whereas above the LCST, 0.02 g/l solutions were investigated. In PVME solution with 1.00 g/l concentration at 50 °C, precipitation was observed within 24 h. PVME does not precipitate from solution with 0.02 g/l concentration.

Intensity of scattered light is sensitive to the molar mass and the size of the scatterers as well as to thermodynamic quality of the solvent and thus can be used to follow the phase separation. Below the LCST, intensity gradually increases upon heating. At the LCST intensity sharply increases and simultaneously increasing R_h indicates the formation of intermolecular aggregates. For solutions of PNIPAM and PVCL homopolymers with concentration below 0.25 g/l, intensity and size of the aggregates reach their maxima at 5–10 °C above the LCST and do not change significantly upon further heating. For PVME it was observed that the aggregates shrink to a certain extent before forming colloidally stable particles, see Fig. 2. The solutions in the range of polymer concentrations between 0.02 and 0.25 g/l are turbid above the LCST. The intensity of light scattered by PNIPAM and PVCL solutions at 50 °C increases linearly with increasing polymer concentration. The distributions of the hydrodynamic radius of the aggregates are monomodal and narrow, see Tables 2 and 3 and discussion below. It is worth mentioning that for all the polymers the change presented in Fig. 2 is completely reversible when the sample is cooled.

Below the LCST, one might expect that water is a thermodynamically good solvent for PVME. This assumes that PVME dissolves as individual chains, similar to PNIPAM. However, scatterers in PVME solutions below as well as above the LCST evidently are too large to represent individual macromolecules of the molar masses studied, see Fig. 2 and Table 4. Mean values of hydrodynamic radius distributions, R_h, suggest that PVME below its LCST is aggregated. This also appears as broad distributions of hydrodynamic radius and existence of an angular dependence of R_h. Thus R_h of corresponding size distributions was of the order of 120 nm at 90° angle for both the PVME samples and 135 and 155 nm at the zero angle for $M_w = 12{,}800$ g/mol and $M_w = 19{,}600$ g/mol respectively. PVME forms aggregates similar to PVCL with molar mass below 100,000 g/mol. However, in contrast to PVCL, in the studied range of scattering angles size distributions of PVME were monomodal. In case of PVCL with molar mass below 100,000 g/mol, a small amount of aggregates was detected using DLS.

Fig. 2(a) qualitatively represents changes in intensity of scattered light, I, and apparent R_h obtained at 90° scattering angle for PVME samples with 1.00 g/l polymer concentration. Solutions were slowly heated and time dependence of intensity was a criterion of equilibrium state. The trend of both dependencies is quite similar to those of PVCL and PNIPAM. Light scattering intensity dramatically increases above the cloud point and the sharp peak in the R_h vs. temperature dependence reveals the formation of large intermolecular aggregates. At higher temperatures aggregates gradually shrink and dense colloidally stable aggregates/mesoglobules are formed above 45 °C. Hydrodynamic radius distributions obtained at 90° scattering angle at 20 and 50 °C for PVME of $M_w = 19{,}600$ g/mol are presented in Fig. 2(b). One can see that size distribution at 50 °C is monomodal and extremely narrow. Weak angular dependence of scattered light was observed in the range of

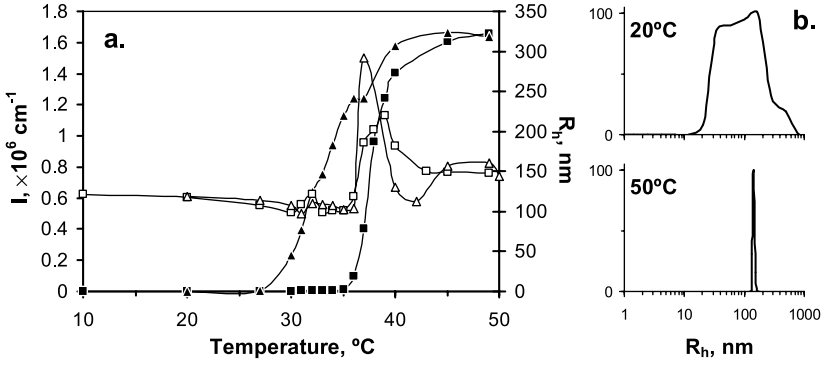

Fig. 2. (a) Temperature dependencies of intensity of scattered light, I, (filled symbols) and apparent hydrodynamic radius, R_h, (open symbols) obtained at 90° scattering angle. Data collected for equilibrium heated PVME of $M_w = 12800$ g/mol (squares) and of $M_w = 19600$ g/mol (triangles) with 1.00 g/l polymer concentration. (b) Corresponding hydrodynamic radius distributions obtained for PVME of $M_w = 19{,}600$ g/mol for selected temperatures above and below the LCST.

scattering angles between 70 and 150°. Absence of angular dependence is typical for solutions of monodisperse homogeneous spheres. For 1.00 g/l PVME solutions, correlation functions are non-exponential below 70°, i.e. decay faster than exponential, owing to the multiple scattering and therefore data analysis is not possible.

To get distributions of hydrodynamic radius, correlation functions were analysed using the inverse Laplace transform algorithm CONTIN. For solutions of PNIPAM, PVCL and PVME above the LCST, mean peak value of hydrodynamic radius distributions calculated with CONTIN, R_h, and radius calculated using the 2ND order cumulant analysis are the same within the experimental error. This R_h is apparent and must be extrapolated to the zero angle and zero concentration. No significant angular dependence of R_h was observed for any of the homopolymers studied in solutions with polymer concentration below 0.25 g/l and in the range of scattering angles between 20 and 150°. These are clear signs of a narrow size distribution. An example of analysis of an intensity correlation function, $G_2(t)$, and corresponding correlation function of electric field, $g_1(t)$, is shown in Fig. 3. Linear dependence of $\ln[g_1(t)]$ vs. time, t, reveals a single exponential decay and thus a narrow size distribution.

No changes in the intensity or in the size of the aggregates formed by PNIPAM and PVCL were observed

Table 2
Light scattering results obtained for PNIPAM solutions at 50 °C

Polymer	c, (g/l)	$(M_w^{agg})^a$, $\times 10^{-9}$ (g/mol)	$(R_g)^b$, (nm)	$(R_h)^c$, (nm)	R_g/R_h	ρ, (g/cm)^3
PNIPAM	0.079	1.3	95	108	0.88	0.40
27,300 g/mol non-	0.059	1.3	94	110	0.85	0.38
equilibrium heated	0.051	1.0	86	105	0.82	0.33
	0.040	0.7	73	91	0.80	0.35
	0.029	0.5	67	81	0.83	0.38
	0.019	0.4	61	79	0.78	0.31
PNIPAM	0.250	0.5	63	86	0.73	0.28
160,000 g/mol	0.120	0.3	51	70	0.74	0.32
non-equilibrium	0.079	0.2	46	62	0.75	0.35
heated	0.059	0.2	44	63	0.69	0.31
	0.050	0.2	42	61	0.69	0.31
	0.046	0.2	41	56	0.73	0.37
	0.040	0.2	43	58	0.74	0.33
	0.034	0.1	40	52	0.76	0.35
	0.030	0.1	38	54	0.70	0.31
	0.025	0.2	46	67	0.69	0.27
PNIPAM	0.10	1.6	100	114	0.88	0.42
160,000 g/mol	0.08	1.5	96	113	0.85	0.40
equilibrium heated	0.06	1.2	82	99	0.83	0.48
	0.05	0.9	86	92	0.93	0.46
	0.04	0.7	73	84	0.87	0.44
	0.02	0.1	39	52	0.76	0.32

[a] Estimated for $dn/dc = 0.20$.
[b] Calculated according to Guinier's method as for a hard sphere.
[c] Apparent value extrapolated to the zero angle.

Table 3
Summary of light scattering data collected at 50 °C for mesoglobules formed by PVCL of M_w = 330,000 g/mol in solutions obtained by consequent dilution of 0.20 g/l solution, see Fig. 7

c, (g/l)	dn/dc, (cm^3/g)	M_w^{agg}, $\times 10^{-9}$ (g/mol)	R_g, (nm)	$(R_h)^a$, (nm)	R_g/R_h	ρ, (g/cm^3)
0.20	0.181[b]	2.5	33[c]	129	0.26	0.47
			102[d]		0.80	
	0.232[e]	1.5	–	–	–	0.29
0.10	0.181[b]	3.4	54[c]	127	0.43	0.65
			110[d]		0.87	
	0.232[e]	2.0	–	–	–	0.40
0.036	0.181[b]	4.4	35[c]	128	0.27	0.84
			120[d]		0.94	
	0.232[e]	2.7	–	–	–	0.51

[a] Apparent value extrapolated to the zero angle.
[b] Measured in water at 20 °C (λ = 514 nm). Literature value is 0.186 cm^3/g (λ = 647 nm) [42].
[c] Calculated according to Zimm's method as for a coil.
[d] Calculated according to Guinier's method as for a hard sphere.
[e] A literature value for collapsed PVCL microgel in water at 40 °C (λ = 532 nm) [43].

during several weeks at 50 °C, see Fig. 4. Both PNIPAM and PVCL form larger particles with increasing initial concentration, i.e. concentration of the solutions prepared at room temperature. However, the mesoglobules of PVCL are larger than those formed by PNIPAM at the same conditions, see Figs. 4 and 5. It is interesting to note that the size of aggregates is not much dependent on the molar mass, which varies radically for the polymers studied.

The effect of annealing on the size of the mesoglobules formed by PNIPAM of 160,000 g/mol is shown in Fig. 6. The heating rate very much determines the size of the resulting particles. The non-equilibrium heating, where samples are quickly brought above the LCST, results in aggregates of smaller size.

Once formed the polymers are trapped inside the mesoglobules as shown by the stability of size and scattering intensity. Furthermore, dilution of the samples with hot water does not induce any changes in apparent R_h of the aggregates, see Figs. 6 and 7. This observation is similar to the one reported earlier for PNIPAM of M_w = (0.5–10) $\times 10^6$ g/mol [15]. Now we see the same phenomenon for PNIPAM with shorter chains and also for PVCL. Moreover, the insets in Figs. 6 and 7 showing $Kc/I_{\theta=90^\circ}$ vs. c plot clearly demonstrate that within the experimental error the second virial coefficient A_2 of the mesoglobules upon dilution is zero. Here K is the optical constant, which is proportional to the square of the increment of refractive index of the polymer, (dn/dc)^2. Therefore, molar masses, M_w, of the aggregates can be estimated from the light scattering measurements at each concentration separately. Accordingly, R_h extrapolated to the zero scattering angle is not an apparent but rather an actual value, meaning that it is not much affected by both intermolecular thermodynamic and hydrodynamic interactions.

To calculate the molar masses of scattering particles, the increment of refractive index, dn/dc, is required. The dn/dc varies with the conformation of macromolecules. Typically for globular structures, such as globular proteins, dn/dc ~ 0.20–0.21. For PVCL at 20 °C and wavelength λ = 514 nm, dn/dc = 0.181 cm^3/g was measured with an Abbe 60/ED refractometer. For comparison, a literature value of dn/dc is 0.186 cm^3/g (λ = 647 nm) [42]. A literature value for collapsed PVCL microgel in water at 40 °C and λ = 532 nm is 0.232 cm^3/g [43]. Unfortunately, it is not possible to determine experimentally dn/dc of the studied homopolymers at temperatures above the cloud points using such low concentrations, i.e. below 0.2 g/l. Therefore dn/dc was estimated using values reported in literature and

Table 4
Light scattering results obtained for equilibrium heated PVME solutions with 0.02 g/l polymer concentration at 50 °C

M_w, (g/mol)	dn/dc, (cm^3/g)	M_w^{agg}, $\times 10^{-9}$ (g/mol)	R_g, (nm)	$(R_h)^a$, (nm)	R_g/R_h	ρ, (g/cm^3)
12800	0.17	0.7	118[b]	150	0.79	0.08
			136[c]		0.91	
	0.20	0.5	–	–	–	0.06
19600	0.17	11.4	148[b]	200	0.74	0.50
			186[c]		0.93	
	0.20	8.2	–	–	–	0.40

[a] Apparent value extrapolated to the zero angle.
[b] Calculated according to Zimm's method as for a coil.
[c] Calculated according to Guinier's method as for a hard sphere.

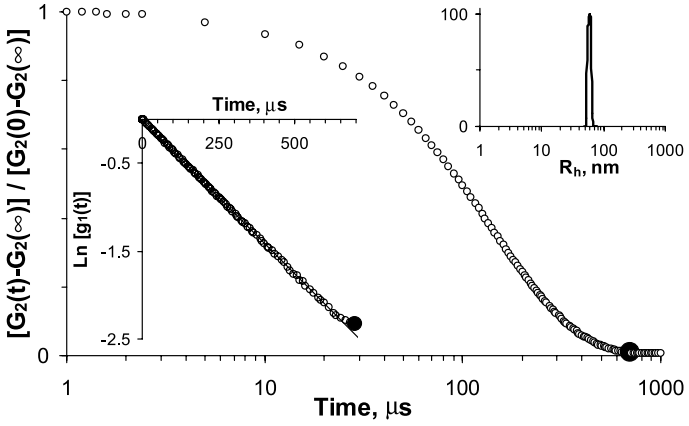

Fig. 3. Analysis of a typical autocorrelation function of scattered light intensity, $G_2(t)$. Correlation function was obtained from a non-equilibrium heated PNIPAM sample of $M_w = 160{,}000$ g/mol with 0.08 g/l polymer concentration at 50 °C and at 90° scattering angle. The lower inset shows a corresponding correlation function of electric field, $g_1(t)$, and the 1st order/linear cumulant fit. Enlarged symbols show the data point corresponding to the same delay time of the functions. The upper inset shows a distribution of hydrodynamic radius, R_h, calculated using CONTIN.

estimation based on these values. Results are presented in Tables 2–4 for PNIPAM, PVCL and PVME respectively. As seen in Tables 3 and 4, though dn/dc affects the molar mass of the aggregates, M_w^{agg}, it has no significant influence on the results.

SLS measurements also enable the determination of radius of gyration, R_g, of the mesoglobules. Together with R_h, the shape and density of the aggregates was estimated. In SLS experiments scattered light intensity was measured between 20 and 150° scattering angles at 50 °C. Experimental data were treated using both Zimm's and Guinier's approach. Assuming the particle shape, the relevant form of the particle scattering function, $P(q) = I(q)/I(q=0)$, was selected. According to Zimm, for macromolecules in a swollen conformation $P(q) = 1 - (q^2 R_g^2)/3$, where $q = (4\pi n_0/\lambda)\sin(\theta/2)$ is the scattering vector, θ is the scattering angle, n_0 is the refractive index of solvent, and λ is the wavelength in vacuum [44]. However, a hard sphere conformation is more likely for mesoglobules. According to Guinier, for large hard spheres when $q^2 R_g^2 \sim 1$, the radius of gyration, R_g, is obtained from $P(q) = \exp[-(R_g^2 q^2)/3]$ [45].

Fig. 8 represents theoretical particle scattering function $P(q) = I(q)/I(q=0)$ for basic particle shapes as a function of parameter x [46], where $x = (2\pi n_0/\lambda)(12R_g^2)^{1/2}\sin(\theta/2)$ for rods, $x = (2\pi n_0/\lambda)(20R_g^2/3)^{1/2}\sin(\theta/2)$ for hard spheres, and $x = (4\pi n_0/\lambda)R_g\sin(\theta/2)$ for coils. Symbols in Fig. 8 show intensities of scattered light normalised to intensity at the zero angle $I(q)/I(q=0)$ plotted vs. parameter x, which was calculated using the experimental R_g from Guinier's analysis for the corresponding shapes. Reciprocal function

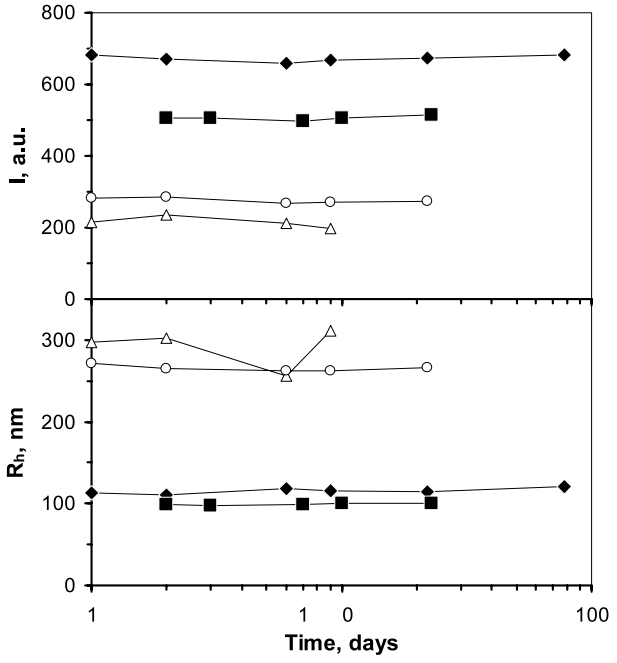

Fig. 4. Intensity of scattered light, I, normalised to intensity from toluene and apparent hydrodynamic radius, R_h, vs. storage time measured at 90° scattering angle for 0.08 g/l polymer solutions at 50 °C: (■) PNIPAM 27300 g/mol, (♦) PNIPAM 160,000 g/mol, (△) PVCL 30,000 g/mol and (○) PVCL 330,000 g/mol. Solutions were equilibrium heated.

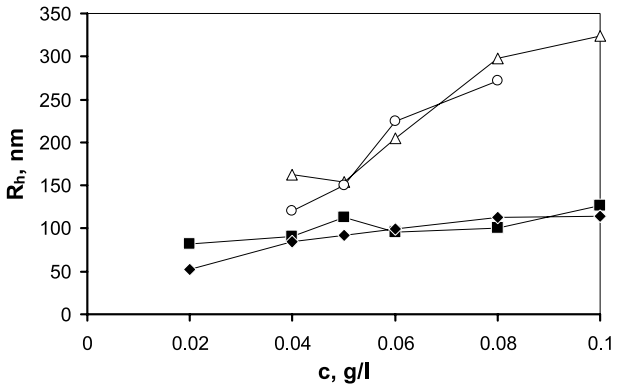

Fig. 5. Apparent hydrodynamic radius, R_h, of equilibrium heated samples with varying concentrations at 90° scattering angle: (■) PNIPAM 27,300 g/mol, (♦) PNIPAM 160,000 g/mol, (△) PVCL 30,000 g/mol and (○) PVCL 330,000 g/mol.

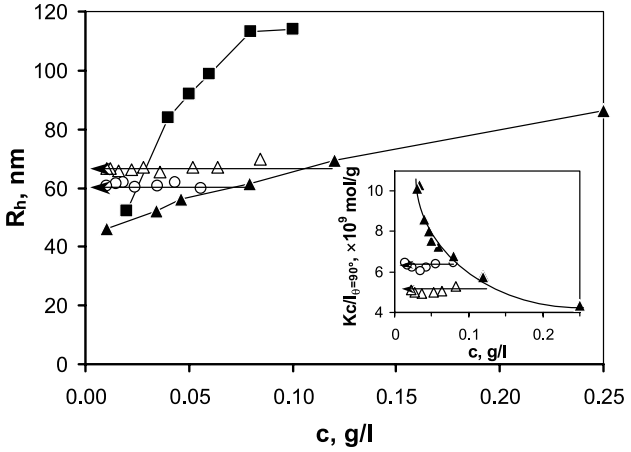

Fig. 6. The effects of the heating rate and dilution with hot water of mesoglobules of PNIPAM 160,000 g/mol on R_h and $Kc/I_{\theta=90^\circ}$: (■) equilibrium heated, (▲) non-equilibrium heated, (△) dilution of 0.12 g/l solution and (○) dilution of 0.08 g/l solution. All the solutions are at 50 °C. $dn/dc = 0.20$ cm^3/g.

$P^{-1}(q)$ vs. $q^2R_g^2$ is shown in the inset. Evidently, the experimental data fit well only the theoretical curve for a hard sphere. Deviation of experimental data from the theoretical curve in the region of the wide angles might be due to a certain degree of polydispersity of the aggregates. However, taking into account the packing density of the mesoglobules ($\rho = 0.35$–0.40) and extremely narrow size distribution of hydrodynamic size, one may expect that mesoglobules are homogeneous non-flowing through spheres with rough surfaces.

Table 2 shows the data for two PNIPAM samples studied. It is seen that R_g and M_w^{agg} change in the same way as R_h. The R_g/R_h ratio, indicative of molecular shape, does not change significantly with polymer concentration and fluctuates around 0.77, the value typical for a homogeneous non-flowing through sphere. Estimated density of the

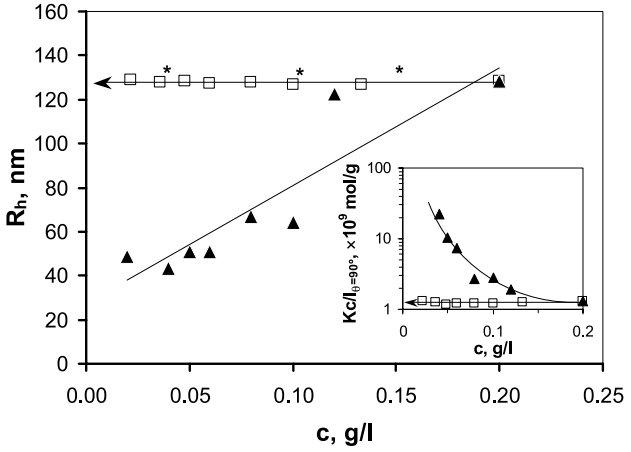

Fig. 7. The effect of concentration on R_h and $Kc/I_{\theta=90^\circ}$ of the mesoglobules (solid triangles) formed upon non-equilibrium heating by PVCL of M_w = 330,000 g/mol and the effect of dilution of 0.20 g/l solution with hot water (open squares). $dn/dc = 0.181$ cm^3/g. All the solutions are at 50 °C. Numerical results for asterisk marked data points are available in Table 3.

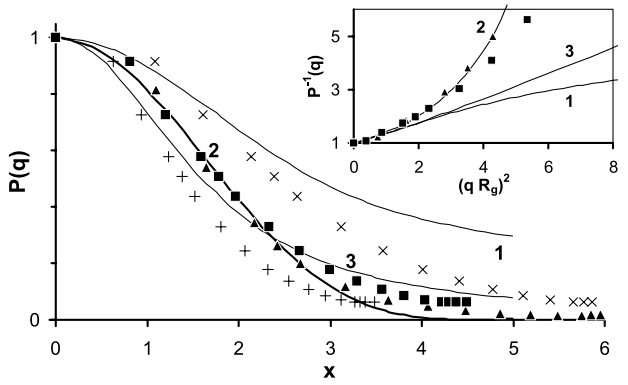

Fig. 8. Theoretical particle scattering function, $P(q)$, for basic particle shapes as a function of parameter x (solid lines): (1) rods, (2) spheres, and (3) coils. Symbols show normalised intensities of scattered light, $I(q)/I(q=0)$, plotted vs. x calculated for the basic shapes using the experimental R_g (Guinier analysis). Data obtained for equilibrium heated PVME of M_w = 12,800 g/mol assuming rod-like shape (×), spherical shape (■), and coil-like shape (+) and of M_w = 19,600 g/mol assuming spherical shape (▲). Both polymers were studied in solutions with 0.02 g/l polymer concentration at 50 °C. Inset shows reciprocal function $P^{-1}(q)$ vs. $(qR_g)^2$.

particles, $\rho = M_w^{agg}/(N_A(4/3)\pi R_h^3)$, shows that particles still contain much water. Such values of R_g/R_h and ρ are typical for polymers in collapsed state and match values reported previously for single chain globules of PNIPAM [10] and PS [47]. Thus for PNIPAM of 10^7 g/mol, $R_g = 20$ nm, R_h = 32 nm, $R_g/R_h = 0.62$ and $\rho = 0.20$ g/cm^3 [10]. Later for the same PNIPAM sample in a fully collapsed state $\rho = 0.34$ g/cm^3 was reported [11]. This value fits well all our observations reported in Tables 2–4 and coincides with theoretically predicted 0.40 g/cm^3 for a space-filling model [48]. As one can also see, the size of the mesoglobules is larger than that of single chain globules. However, single chain globules of PNIPAM were observed at significantly lower polymer concentrations (~0.005 g/l) and at higher concentrations might form stable multimolecular aggregates, i.e. mesoglobules.

It was interesting to see if the PNIPAM samples of two different molar masses form similar mesoglobules of different size under various external conditions, i.e. polymer concentration and heating rate. To do that, fractal dimensionality of mesoglobules was determined. Experimental conditions, under which mesoglobules were formed, were the same as in Table 2. Scaling of the molar mass of PNIPAM mesoglobules M_w^{agg} with $R_g^{2.7}$ is presented in Fig. 9. Obviously, various mesoglobules follow the same power law $M_w^{agg} \propto R_g^{2.7}$. This means that external conditions and molar mass of individual chains do not influence the internal structure and shape of mesoglobules. Fractal dimension 2.7 is smaller than for hard spheres (i.e. $M \propto R_g^3$), showing that the mesoglobules are not fully packed and the dimension is significantly larger than that for coils (i.e. $M \propto R_g^2$). This observation entirely excludes a cylindrical conformation predicted theoretically for amphiphilic polymers [33]. Packing density presented in Table 2

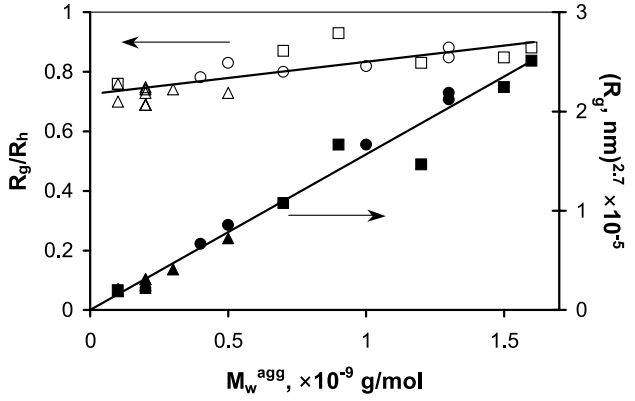

Fig. 9. Scaling of molar mass of PNIPAM mesoglobules M_w^{aag} vs. their radius of gyration R_g with fractal dimension of 2.7 (filled symbols) and the shape factor R_g/R_h (open symbols). Conditions, at which mesoglobules were formed, correspond to Table 2: M_w = 27,300 g/mol, non-equilibrium heated (circles); M_w = 160,000 g/mol, non-equilibrium heated (triangles); M_w = 160,000 g/mol, equilibrium heated (squares).

does not change with M_w^{agg}, which follows nicely the scaling concept. The shape factor R_g/R_h is also presented in Fig. 9. R_g/R_h increases slightly with M_w^{agg}. Such an increase is expected for a particle with a rough surface.

Results obtained for PVCL mesoglobules are similar to those for PNIPAM. It is easy to see from Table 3 that Zimm's method is not appropriate and gives misleading values of R_g and R_g/R_h.

Table 4 represents light scattering results obtained for 0.02 g/l PVME solution at 50 °C. Angular dependence of mean R_h was not significant and the values presented in Table 4 are extrapolated to the zero angle. All distributions of the hydrodynamic size were monomodal and narrow in the studied range of angles. As in the cases with PVCL and PNIPAM, R_g and $I(q=0)$ were calculated from the angular dependence of intensity of scattered light using Zimm's and Guinier's methods and molar mass of aggregates M_w^{agg} was estimated assuming zero second virial coefficient A_2 and estimated dn/dc values. As one can clearly see, aggregates of PVME at 50 °C are dense spheres. Again, the Guinier approach gives realistic data whereas Zimm's method does not.

Thus we may conclude that all the three studied homopolymers form colloidal aggregates/mesoglobules in aqueous solutions above their cloud point and the experimental results obtained using light scattering obey the theoretical prediction for homogeneous spheres. By dilution of the samples it was shown that the density, although affected by the estimated dn/dc value, gives values typical for rather dense particles. The second virial coefficient A_2 of the mesoglobules is zero.

Recently, we have studied amphiphilic diblock copolymers PNIPAM-*b*-PS and PNIPAM-*b*-P*t*BMA in aqueous solutions [38]. These copolymers form micellar aggregates in water at room temperature when transferred from an organic solvent. However, the colloidal stability of the aggregates at elevated temperature could not be satisfactorily understood. Actually, properties of PNIPAM-*b*-PS and PNIPAM-*b*-P*t*BMA in aqueous solutions heated above the LCST of PNIPAM resemble those of PNIPAM homopolymer. The hydrophobic blocks are long enough to form a dense core and force the PNIPAM blocks to organise in a particle shell. One may expect that only the PNIPAM blocks define the solution properties of the polymeric micelles. The micelles are colloidally stable and precipitation at elevated temperature did not occur even upon prolonged heating at 50 °C for several days. Apparent radii of the polymeric micelles at 20 °C were R_h = 38 nm for PNIPAM-*b*-PS and 61 nm for PNIPAM-*b*-P*t*BMA and at 40 °C R_h were 33 and 55 nm, correspondingly. Static light scattering on polymeric micelles in water yields apparent molar masses for the aggregates, which were at room temperature 10×10^6 g/mol for PNIPAM-PS and 164×10^6 g/mol for PNIPAM-tBMA. At 40 °C, molar masses were 15×10^6 and 184×10^6 g/mol.

The larger aggregates of PVCL and PVME compared to the aggregates of PNIPAM are probably due to different thermal transition behaviour. For PVME and especially for PVCL the calorimetrically detected transition around LCST is much broader than that for PNIPAM, see Fig. 10. The different thermal transition behaviour arises from the

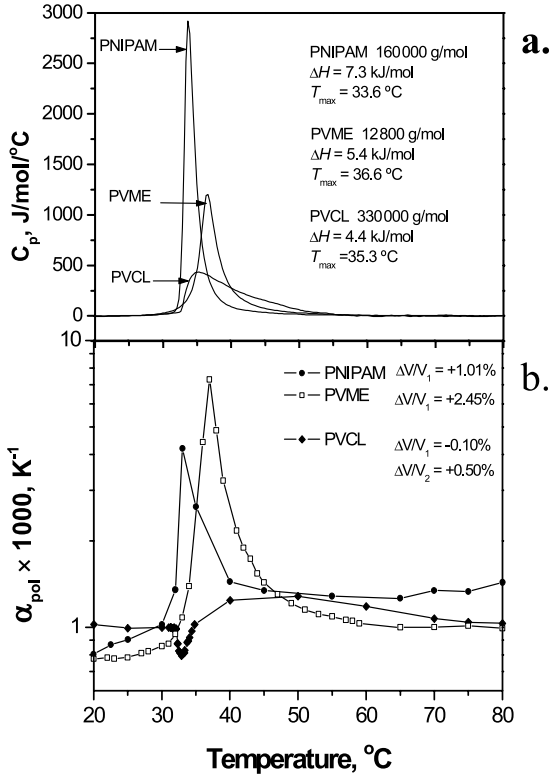

Fig. 10. (a) Microcalorimetric endotherms for solutions of PNIPAM (1.00 g/l), PVCL (1.00 g/l), and PVME (5.00 g/l) in H_2O. Heating rate was 60 °C/h. (b) Temperature dependence of the coefficient of thermal expansion, α_{pol}, of PNIPAM, PVME-12,800, and PVCL-330,000 in water; polymer concentration: 5.00 g l^{-1}.

different chemical composition of these polymers and results in the classification to the different types (type I, II, and III, Section 1). Regardless of these obvious differences in calorimetric behaviour, these three polymers form similar stable aggregates.

When an aqueous solution of thermally responsive polymer is heated above the cloud point temperature, dehydration of the polymer chain takes place. In the cases of PNIPAM, PVCL, and PVME, the dehydration is an endothermic process, and thus, it could be followed by a microcalorimeter. The changes with temperature of the partial excess heat capacity C_p of aqueous solutions of PNIPAM, PVCL, and PVME are presented in Fig. 10(a). In order to compare different polymers, heat capacities were normalized per molar content of repeating units. The thermograms are distinctly different. For PNIPAM, the endothermic transition takes place in a very narrow temperature range and the heat of the transition, ΔH, is the highest, 7.3 kJ/mol of NIPAM units. PVCL has a broad, and markedly asymmetric endothermic peak, with a sharp increase in heat capacity on the low temperature side and a gradual decrease of the heat capacity at temperatures higher than the maximum temperature T_{max}. The heat of transition for PVCL is small compared to PNIPAM, i.e. 4.4 kJ/mol. The endotherm of PVME is also broad but rather symmetric. The total heat of the transition is 5.4 kJ/mol. The transitions observed are completely reversible.

The cloud point temperatures for aqueous solutions of PVCL and PNIPAM are closely related to the onset temperature of the endothermic peak in a thermogram. Determination of the onset temperature for PVME is rather inaccurate due to the broadness of the peak. And actually in the PVME case, the cloud point, 36.0 °C, is close to the maximum temperature of the thermogram, T_{max} in Fig. 10(a). In all three cases, the endothermic transition is over at temperatures above 50 °C.

Pressure perturbation calorimetry, PPC, measurements were performed on PNIPAM, PVCL and PVME. From the PPC measurement, the coefficient of thermal expansion, α_{pol}, of the polymer is obtained. The temperature dependence of α_{pol} over a broad temperature range was investigated. It should be noted that $\alpha_{pol}(T)$ reflects the changes in the partial specific volume of the polymer, $\bar{V}_{pol}$, and not simply the expansion of the intrinsic volume of the polymer chain. The partial specific volumes of the polymers were determined by an increment method based on the group contribution theory developed to estimate $\bar{V}$ of aqueous systems and estimated to be accurate within 2% [49]. Thus, for PVCL, $\bar{V} = 0.834$ cm^3/g, for PNIPAM, $\bar{V} = 0.894$ cm^3/g, and for PVME, $\bar{V} = 0.856$ cm^3/g.

The dependence of coefficient of thermal expansion on temperature is presented for different polymers in Fig. 10(b). The general shape of the curves for PNIPAM and PVME resembles each other. There is a large positive peak at the same temperature range as the endothermic transition occurs. For PVCL, the transition is more complicated and it is composed of two subsequent peaks: first $\alpha_{pol}(T)$ undergoes a sharp decrease, reaches a minimum, then increases abruptly with increasing temperature to reach a maximum value for $T \sim 45$ °C and gradually decreases as the temperature further increases. By integrating $\alpha_{pol}(T)$, with respect of temperature, we obtain the relative change of the partial specific volume of polymer, $\Delta V/V$, at the transition range.

If the baseline is not subtracted, a negative change in heat capacity due to the transition can be detected. The value of ΔC_p was the same for all polymers within the experimental error, i.e. -65 ± 10 J/mol^{-1} °C. A similar negative change in C_p has been observed also for the phase transitions of various pluronic-type block copolymers [50]. Such a negative heat capacity change during the phase transition may be taken as an indication of diminished interaction between water molecules and polymer chains.

4. Discussion and conclusions

Thermosensitive homopolymers PNIPAM, PVCL and PVME in dilute aqueous solutions below 0.25 g/l were investigated above the LCST. Despite a significant difference between the polymers, they form similar colloidally stable aggregates, mesoglobules, with no stabilizing agent added. The particles are spherical and have a very narrow size distribution. The size of the formed particles depends on the initial concentration and the heating rate of the solutions and is not significantly affected by the molar mass of individual macromolecules. Thus, for PNIPAM samples of two different molar masses, the fractal dimension of mesoglobules was 2.7 independently on the conditions at which mesoglobules were formed. Once being formed, the particles neither precipitate nor disintegrate upon dilution. The second virial coefficient for the mesoglobules is zero, which demonstrates a balance of all interactions in solution. The size of mesoglobules did not change at least for several weeks, showing the absence of any significant association of mesoglobules.

The formation of mesoglobules was shown for three different thermosensitive homopolymers and therefore it most likely is a universal phenomenon and may be suggested to have an entropic origin. In a thermodynamically poor solvent, individual macromolecules associate decreasing the overall entropy of the solution. Aggregation stops when the entropy loss balances the potential energy of a new metastable state at elevated temperature. Narrow size distributions of the mesoglobules also suggest entropic origin of the intermolecular association. The entropic approach explains the effect of polymer concentration on the size of the intermolecular aggregates; the higher polymer concentration, the larger loss of entropy is required to balance the larger energy of the phase transition. This results in larger aggregates formed. Existence of hydrophilic groups is an additional, though not a major factor of

stabilisation. However, the entropic approach does not explain the effect of the heating rate on the size of the formed particles.

The stability of the dispersions upon dilution at 50 °C and zero value of the osmotic second virial coefficient suggest that the surface of the particles at temperatures above the LCST may possess a hydrophilic character. The macromolecules self organise and build up particles with the polar groups turned towards the surrounding aqueous phase. In this respect, a cylindrical conformation predicted theoretically for amphiphilic polymers [33] is preferable owing to the large surface to volume ratio. However, the existence of a cylindrical mesoglobule has not been observed in our experiments. Mesoglobules of PNIPAM, PVCL and PVME are spherical, similar to single chain globules [10,11]. Apparent disagreement with theoretical expectation may come from the following reasons. Associating cylindrical globules may form spherical particles observed in experiment. On the other hand, surface of mesoglobules may be rather rough, thus increasing the area of contact with water molecules.

Molar mass of individual chains appears to have no significant influence on the size of mesoglobules, which is demonstrated in Fig. 5. On the other hand, the size of mesoglobules depends on the heating rate, which might indicate the importance of the dynamics of chain aggregation. However, the dynamics should depend on the chain length, which has not been observed. This experimental finding is somewhat confusing and must be studied more in detail. The observation of multimolecular aggregates does not rule out the possibility of thermosensitive polymers of high molar mass to adopt a single chain globular conformation, colloidally stable above the cloud point in extremely dilute solutions. In other words, one may expect that under certain external conditions (heating rate, polymer concentration etc.), long polymer chains form single molecule globules whereas shorter chains associate forming mesoglobules with the same fractal dimension 2.7.

As for the core-shell polymeric micelles formed by dihydrophilic block copolymers of PNIPAM, it is evident that both blocks of the diblock copolymers are hydrophobic above the LCST of PNIPAM. PNIPAM totally screens the highly hydrophobic PS and P*t*BMA and controls solution properties of the micelles below and above the LCST. It seems natural to expect that stabilisation of the micelles above the LCST has the same origin as that of the PNIPAM homopolymer.

The resistance of mesoglobules to association can be attributed to the viscoelastic effect, recently discussed in literature [51]. Thus, the stability of dispersions can be understood in terms of the characteristic time between a collision of two globules and the time of reptation of the chain on the globule surface [52]. For the standard diffusion-limited aggregation process, two globules merge every time they collide in the course of Brownian motion. Under the conditions of the experiment on the coil-to-globule transition of PS in cyclohexane [53], time of collision was of the order of 0.1 s, whereas actual aggregation started only after about 10 min. Globules in poor solvent may collide several thousands of times before merging takes place [52]. A recent review by Baysal and Karasz on the collapse of flexible macromolecules in organic solvents unambiguously demonstrates that the lifetime of single-chain globules without significant precipitation is much longer than the time of collisions, which allows studies of kinetics of the transition [54]. A slow aggregation also was reported for PNIPAM above the LCST [10].

To explain such a slow process of aggregation, Tanaka introduced an ‘entanglement force’ operational on the prereptational time scale [52]. Accordingly, merging of two globules proceeds via reptation. However, the globules approaching each other are dense, highly entangled and intraglobular mobility/viscoelasticity is limited, which results in topological restrictions on a time scale shorter than the time of reptation, i.e. the time required to establish a permanent chain entanglement. No entropy can be gained due to topological prohibition of the majority of conformations and merging is entropically unfavourable. Therefore, before the reptation may take place, the globules experience an entropic counterforce, topological repulsion, called an ‘entanglement force’. Rough estimation showed that work of $\sim 10 k_B T$ is needed to overcome the entanglement force and slow down the aggregation. Numerous collisions of globules happen before an effective entanglement may occur.

When two core-shell particles discussed in this article collide with each other above the LCST of PNIPAM, the time of collision is much shorter than the reptation time of the copolymer chains inside each micelle. The reptation of the copolymer chains are extremely slow, not only because the PNIPAM blocks are in a collapsed state, but mainly owing to the strong hydrophobic interaction among the PS or P*t*BMA blocks in the core [55]. In view of that, two particles behave like tiny hard spheres and the collision is elastic. One may say that the highly hydrophobic blocks act as stabilising agents. The clear supportive evidence is that the hydrophobically modified PNIPAM copolymer can form smaller mesoglobules than its homopolymer with a similar length and the aggregation number dramatically decreases as the hydrophobic content increases, which might be against our expectations, but can be well explained in terms of the viscoelastic effect [51].

The glassy state of the polymers in the mesoglobular phase may be an additional factor affecting the mechanism of stability against precipitation. Thus for the hydrophobic blocks in the core, glass transition temperatures are 106 and 107 °C for PS and 118 °C for P*t*BMA [38]. These are much higher than the range of temperatures studied and demonstrate that reptation of the block copolymers out of the core is restricted. As for the thermosensitive blocks and homopolymers, the collapse of a macromolecule results in increasing density of polymeric material within the globule,

which may end up in vitrification. The $T_g = 145$ °C for PVCL [4] and $T_g = 133$–137 °C for PNIPAM [38,56] in bulk. The T_g of both polymers decreases with increasing water content due to the plasticizing effect of water and intersects with the diagram of state roughly at 40–50 °C and a polymer weight fraction of ~0.8–0.9. These values are high in comparison to ρ in Tables 2–4. However, one should remember that ρ was estimated assuming homogeneous distribution of polymeric material. Fractal dimension of 2.7 and the R_g/R_h values presented in Fig. 9 and the static structure factor in Fig. 8 suggest a complex morphology of mesoglobules, e.g. foam-like morphology formed by the polymer in glassy state. In our microcalorimetric experiments we did not notice any evidence of the glass transition. However, Van Mele et al. have recently demonstrated the possibility of partial vitrification of PNIPAM in the polymer-rich phase above its LCST using modulated temperature DSC [57,58] For PVME, $T_g = -19$ °C for the completely dry sample [6] or ranges between −82 and −22 °C [56] and decreases with decreasing polymer content in the water-polymer mixture. This leaves the glass transition temperature out of discussion and allows one to expect a pure viscoelastic mechanism of stabilisation of PVME mesoglobules.

Acknowledgements

The work was supported by INTAS (Project 01-607). O. Confortini acknowledges the ESF-programme STIPOMAT for the research grant. Authors are grateful to Prof W. Burchard and Prof H. Berghmans for fruitful discussions.

References

[1] Schild HG. Prog Polym Sci 1992;17:163–249.
[2] Afroze F, Nies E, Berghmans HJ. Mol Struct 2000;554(1):55–68.
[3] Kirsh YE. Water soluble poly-*N*-vinylamides. Synthesis and physicochemical properties. Chichester: Wiley; 1998.
[4] Meeussen F, Nies E, Berghmans H, Verbrugghe S, Goethals E, Du Prez F. Polymer 2000;41(24):8597–602.
[5] Nishi T, Kwei K. Polymer 1975;16(4):285–90.
[6] Meeussen F, Bauwens Y, Moerkerke R, Nies E, Berghmans H. Polymer 2000;41(10):3737–43.
[7] Maeda H. J Polym Sci, Part B: Polym Phys 1994;32:91–7.
[8] Maeda H. Macromolecules 1995;28(14):5156–9.
[9] Schäfer-Soenen H, Moerkerke R, Berghmans H, Koningsveld R, Dušek K, Šolc K. Macromolecules 1997;30(3):410–6.
[10] Wu C, Zhou S. Macromolecules 1995;28(15):5388–90. Wu C, Zhou S. Macromolecules 1995;28(24):8381–7.
[11] Wang X, Qiu X, Wu C. Macromolecules 1998;31(9):2972–6.
[12] Lau ACW, Wu C. Macromolecules 1999;32(3):581–4.
[13] Lebedev V, Török Gy, Cser L, Treimer W, Orlova D, Sibilev AJ. Appl Cryst 2003;36(4):967–9.
[14] Lebedev VT, Török Gy, Cser L, Kali Gy, Kirsh YE, Sibilev AI, et al. Physica B 2001;297:50–4.
[15] Gorelov AV, Du Chesne A, Dawson KA. Physica A 1997;240:443–52.
[16] Dawson KA, Gorelov AV, Timoshenko EG, Kuznetsov YA, Du Chesne A. Physica A 1997;244:68–80.
[17] Chan K, Pelton R, Zhang J. Langmuir 1999;15(11):4018–20.
[18] Timoshenko EG, Kuznetsov YA. arXiv.org e-Print: Cond. Mat. 2000; arXiv:cond-mat/0011386.
[19] Timoshenko EG, Kuznetsov YA. J Chem Phys 2000;112(18):8163–75.
[20] Timoshenko EG, Kuznetsov YA. Prog Colloid Polym Sci 2000;115:117–20.
[21] Virtanen J, Baron C, Tenhu H. Macromolecules 2000;33(2):336–41.
[22] Virtanen J, Tenhu H. Macromolecules 2000;33(16):5970–5.
[23] McPhee W, Tam KC, Pelton R. J Colloid Interf Sci 1993;156:24–30.
[24] Deng Y, Pelton R. Macromolecules 1995;28(13):4617–21.
[25] Lozinsky VI, Simenel IA, Kulakova VK, Kurskaya EA, Babushkina TA, Klimova TP, et al. Macromolecules 2003;36(19):7308–23.
[26] Qiu X, Kwan CMS, Wu C. Macromolecules 1997;30(20):6090–4.
[27] Siu MH, Cheng He C, Wu C. Macromolecules 2003;36(17):6588–92.
[28] Khokhlov AR, Khalatur PG. Physica A (Amsterdam) 1998;249:253–61.
[29] Khokhlov AR, Khalatur PG. Phys Rev Lett 1999;82(17):3456–9.
[30] Berezkin AV, Khalatur PG, Khokhlov ARJ. Chem Phys 2003;118(17):8049–60.
[31] Lau KF, Dill KA. Macromolecules 1989;22(10):3986–97.
[32] Baulin VA, Zhulina EB, Halperin AJ. Chem Phys 2003;119(20):10977–88.
[33] Vasilevskaya VV, Khalatur PG, Khokhlov AR. Macromolecules 2003;36(26):10103–11.
[34] Laukkanen A, Valtola L, Winnik FM, Tenhu H. Macromolecules 2004;37(6):2268–74.
[35] Vihola H, Laukkanen A, Valtola L, Hirvonen J, Tenhu H. Biomaterials 2005;26(16):3055–64.
[36] Verdonck B, Goethals EJ, Du Prez F. Macromol Chem Phys 2003;204(17):2090–8.
[37] Reyntjens W, Goethals EJ. Des Monomers Polym 2001;4(2):195–201.
[38] Nuopponen M, Ojala J, Tenhu H. Polymer 2004;45(11):3643–50.
[39] Brown W, editor. Dynamic light scattering. The method and some application. Oxford: Clarendon Press; 1993.
[40] Kujawa P, Winnik F. Macromolecules 2001;34(12):4130–5.
[41] Lin LN, Brandts JF, Brandts M, Plotnikov V. Anal Biochem 2002;302(1):144–60.
[42] Eisele M, Burchard W. Makromol Chem 1990;191:169–84.
[43] Gao Y, Au-Yeung SCF, Wu C. Macromolecules 1999;32(11):3674–7.
[44] Evans JM. In: Huglin MB, editor. Manipulation of light scattering data. Light scattering from polymer solutions. London: Academic Press; 1972. p. 89–164.
[45] Porod G. In: Glatter O, Kratky O, editors. General theory. Small angle X-ray scattering. London: Academic Press; 1982. p. 17–51.
[46] Kratochvil P. In: Huglin MB, editor. Particle scattering functions. Light scattering from polymer solutions. London: Academic Press; 1972. p. 333–84.
[47] Sun ST, Nishio I, Swislow G, Tanaka TJ. Chem Phys 1980;73(12):5971–5.
[48] Marchetti M, Prager S, Cussler EL. Macromolecules 1990;23(14):3445–50.
[49] Zana RJ. J Polym Sci, Polym Phys Ed 1980;18:121–6.
[50] Beezer AE, Loh W, Mitchell JC, Royall PG, Smith DO, Tute MS, et al. Langmuir 1994;10(11):4001–5.
[51] Wu C, Li W, Zhu XX. Macromolecules 2004;37(13):4989–92.
[52] Chuang J, Grosberg AY, Tanaka TJ. Chem Phys 2000;112(14):6434–42.
[53] Chu B, Ying Q, Grosberg AY. Macromolecules 1995;28(1):180–9.

[54] Baysal BM, Karasz FE. Macromol Theory Simul 2003;12(9):627–46.
[55] Remark by the anonymous reviewer.
[56] Brandrup J, Immergut EH, Grulke EA, editors. Polymer handbook. 4th ed. New York: Wiley; 1999.
[57] Van Durme K, Verbrugghe S, Du Prez FE, Van Mele B. Macromolecules 2004;37(3):1054–61.
[58] Van Durme K, Van Assche G, Van Mele B. Macromolecules 2004; 37(25):9596–605.